Pflugers Arch - Eur J Physiol
DOI 10.1007/s00424-008-0558-6

Regulation of the murine TRPP3 channel by voltage, pH, and changes in cell volume

Takahiro Shimizu · Annelies Janssens · Thomas Voets · Bernd Nilius

Received: 16 April 2008 / Revised: 8 July 2008 / Accepted: 10 July 2008

Abstract Transient receptor potential (TRP) polycystin 3 (TRPP3) is a member of the TRP superfamily of cation channels. Murine TRPP3 has been reported to form an acid-activated cation channel on the plasma membrane when coexpressed with the polycystin 1-like protein 3 (PKD1L3); however, the function and biophysical properties of TRPP3-dependent channels have not yet been characterized in detail. Here we show that overexpression of murine TRPP3 channel in HEK293 cells, without coexpression of PDK1-like proteins, leads to robust channel activity. These channels exhibit a high single-channel conductance of 184 pS at negative potentials, are Ca^{2+}-permeable, and relatively nonselective between cations. Whole-cell experiments showed a characteristic form of voltage-dependent gating of TRPP3 channels, whereby repolarization after depolarization caused large transient inward TRPP3 tail currents. Moreover, we found that TRPP3 activity was increased upon cell swelling and by alkalization. Taken together, our results demonstrate that TRPP3, on its own, can act as a voltage-dependent, pH- and volume-sensitive plasma membrane cation channel.

Keywords Transient receptor potential channels · Polycystins · Murine TRPP3 · Voltage dependency · Volume sensitivity · pH sensitivity

Introduction

Transient receptor potential (TRP) channels constitute a superfamily of nonselective cation channels. Some, if not all, members of the TRP superfamily are sensitive to multiple stimuli such as temperature, taste compounds, and mechanical and osmotic stress [18, 23, 28]. The transient receptor potential polycystin (TRPP) channels form one of the subfamilies of the TRP cation channel superfamily and includes three homologous members: TRPP2 [also called polycystin-2 (PC2) or polycystic kidney disease-2 (PKD2)], TRPP3 [polycystin-L (PCL) or PKD2-like 1 (PKD2L1)], and TRPP5 (PKD2L2) [5, 18, 28]. Although TRPP2 and TRPP3 have been reported to be functional Ca^{2+}-permeable nonselective cation channels [1, 7], activities of these channels seem to be modulated by TRPP1 (polycystin-1 or PKD1) and/or TRPP1-like proteins.

TRPP1 and its homologues are not considered TRP channels because of their specific structure with 11 transmembrane-spanning helices (compared to the six transmembrane segments in each TRP channel subunit) and are assumed to function as receptors or scaffolding proteins [4, 10, 17, 22]. For example, TRPP1 and TRPP2 form a receptor-ion channel complex, and mutations in both TRPP1 and TRPP2 cause autosomal dominant polycystic kidney disease (ADPKD) [24]. TRPP3 has recently been proposed to form a putative sour receptor complex in taste cells when coexpressed with PKD1L3, one of TRPP1-like proteins [9, 10, 15]. Based on the TRPP3 expression pattern in a diversity of tissues [21], however, the TRPP3 channels

Electronic supplementary material The online version of this article (doi:10.1007/s00424-008-0558-6) contains supplementary material, which is available to authorized users.

T. Shimizu · A. Janssens · T. Voets · B. Nilius (✉)
Department of Molecular Cell Biology,
Laboratory of Ion Channel Research,
Katholieke Universiteit Leuven,
Campus Gasthuisberg, Herestraat 49, Bus 802,
B-3000 Leuven, Belgium
e-mail: bernd.nilius@med.kuleuven.be

might also sense other physiological stimuli. We have therefore studied the regulatory mechanisms of TRPP3 channel activity.

Human TRPP3 has been reported to form a constitutively active nonselective cation channel with a large single-channel conductance and significant Ca^{2+} permeability in the *Xenopus* oocytes expression system [1]. It has been shown that TRPP3 channels are voltage-dependent [13] and inhibited by monovalent cations larger than tetraethyl ammonium [2] as well as by multivalent cations such as Mg^{2+}, Gd^{3+}, and La^{3+} [1, 14]. In the case of murine TRPP3, however, neither the single-channel conductance nor the exact gating properties have been investigated so far. A previous report suggested that TRPP3 is activated by strong acidification in mammalian cells when coexpressed with PKD1L3 [10]. Therefore, it is also noteworthy evaluating electrophysiological properties of murine TRPP3 channels itself.

In the present study, we characterized channel activity of TRPP3 upon overexpression in human embryonic kidney (HEK293T) cells. We show that, even in the absence of TRPP1-like proteins, murine TRPP3 forms spontaneously active nonselective cation channels in the plasma membrane, which are sensitive to voltage and osmotically induced cell volume changes.

Materials and methods

Cell culture and transfection

Human embryonic kidney cells, HEK293T, were grown in Dulbecco's modified Eagle's medium supplemented with 10% (*v*/*v*) fetal calf serum, 2 mM L-glutamine, 2 U/ml penicillin, and 2 mg/ml streptomycin at 37°C in a humidity-controlled incubator with 10% CO_2. HEK293T cells were transiently transfected with the murine TRPP3 gene (kindly provided by Dr. H. Matsunami, Duke University Medical Center) subcloned in the bicistronic pCINeo-IRES-GFP vector [26] using a Mirus TransIT-293 transfection reagent (Mirus, Madison, WI, USA) according to the manufacturers' instruction. All experiments were carried out more than 36 h after transfection.

Electrophysiology

Whole-cell and cell-attached recordings were performed with an EPC-9 patch-clamp amplifier (HEKA Electronik, Lambrecht, Germany) at room temperature. Patch master software (HEKA Electronik) was used for command pulse control and data acquisition, and WinASCD software (provided by Dr. G. Droogmans, KU Leuven, Leuven, Belgium ftp://ftp.cc.kuleuven.ac.be/pub/droogmans/winascd.zip) was utilized for data analysis. Currents were filtered at 3 kHz and digitalized at 10 kHz. Patch electrodes had a resistance of 2–3 MΩ when filled with pipette solution. Liquid junction potential at the tip of the electrodes was calculated with PClamp 9.2 software (14.9 mV: Molecular Devices, Foster City, CA, USA) and compensated with the Patch master software. The access resistance (<10 MΩ) was electrically compensated by 70% to minimize voltage errors. Salt bridges containing 3 M KCl were employed to minimize junction potential changes at the reference electrode in ion selectivity experiments.

The relative permeability for monovalent cations, compared to Na^+, was calculated using the following equation; $P_X/P_{Na} = (\gamma_{Na} \times [Na^+]_0/\gamma_X \times [X]_0) \times \exp(\Delta V_{rev} \times F/RT)$, where ΔV_{rev} is $E_{rev,X}-E_{rev,Na}$, F and R are universal constants, and T is the absolute temperature (293.15 K corresponding to 20°C). γ_{Na} and γ_X are activity coefficients for Na^+ and other monovalent cations, respectively. For Ca^{2+} selectivity, we used the following equation; $P_{Ca}/P_{Cs} = \left(\gamma_{Cs} \times [Cs^+]_i/4 \times \gamma_{Ca} \times [Ca^{2+}]_0\right) \times \exp(\Delta V_{rev} \times F/RT) \times \{1 + \exp(\Delta V_{rev} \times F/RT)\}$, where ΔV_{rev} is $E_{rev,Ca}-E_{rev,Na}$, γ_{Cs} (0.76) and γ_{Ca} (0.3) are the activity coefficient for Cs^+ and Ca^{2+}, respectively [8]. To obtain P_{Ca}/P_{Na}, P_{Ca}/P_{Cs} was multiplied by P_{Cs}/P_{Na}. For details of equations, see a previous manuscript [12].

The amplitude of single-channel currents was measured as the peak-to-peak distance in Gaussian fits of amplitude histograms. Channel activity (NP_o, where N is the number of channels and P_o is the open probability) at −60 mV was calculated by dividing the mean current amplitude of recordings lasting longer than 30 s by the single-channel amplitude obtained from the same traces.

The pipette (intracellular) solution (290 mosmol/kg H_2O) in whole-cell recordings consisted of (in mM): 130 Cs-aspartate, 2 MgATP, 10 $MgCl_2$, 1 ethylene glycol tetraacetic acid (EGTA), 10 4-(2-hydroxyethyl)-1-piperazineethanesulfonic acid (HEPES), buffered at pH 7.3 with CsOH. To prevent contamination by endogenous Mg^{2+}-inhibitable cation currents, this high-Mg^{2+} pipette solution was utilized in all patch-clamp experiments. In some experiments, to investigate the Ca^{2+} dependency of TRPP3 currents, EGTA was increased to 10 mM, either without added Ca^{2+} or with addition of $CaCl_2$ to obtain a free Ca^{2+} concentration of 1 μM. The free Ca^{2+} concentration was calculated with WCabuf software (provided by Dr. G. Droogmans, KU Leuven, Leuven, Belgium). The standard isotonic bathing solution (300 mosmol/kg H_2O) contained (in mM): 130 NaCl, 1 $MgCl_2$, 10 HEPES, 40 mannitol, buffered at pH 7.4 with NaOH. This solution was also utilized as pipette solution in cell-attached recordings. For

ion selectivity experiments, $MgCl_2$ was omitted from the standard solution, and 5 mM ethylenediaminetetraacetic acid was added. NaCl was replaced with CsCl or *N*-methyl-D-glucamine (NMDG)–Cl in an equimolar fashion. For determining Ca^{2+} selectivity, 65 mM $CaCl_2$ was used instead of 130 mM NaCl, and 65 mM mannitol was added to compensate the osmolality. To test for acid sensitivity of voltage-dependent activity of murine TRPP3 channels, NaCl in the standard solution was replaced equimolarly with Na-gluconate to prevent contamination by acid-activated Cl^- currents [11], and 25 mM citric acid was added just before use, which resulted in pH 2.7. To check the effect of alkalization (pH 9), 10 mM *N*-Tris(hydroxymethyl)methyl-3-aminopropanesulfonic acid (TAPS) was added to the standard solution. Cell swelling and shrinkage was carried out using hypotonic (260 mosmol/kg H_2O) and hypertonic (350 mosmol/kg H_2O) solutions made by changing the concentration of mannitol in the standard isotonic solution. The osmolality was measured with a vapor pressure osmometer (model 5500; Wescor, Logan, UT, USA).

Single-cell size measurements

Single-cell size measurements were performed in whole-cell patch-clamped HEK293T cells overexpressing TRPP3. Cell images were visualized through a CCD camera (TVCCD-200: Monacor, Bremen, Germany), captured with a generic video capture PCI card, and recorded every 15 s using InterVideo WinDVR (Corel, ON, Canada). The cross-sectional area (CSA) of targeted cells was analyzed using ImageJ software (version 1.38x: freeware at http://rsb.info.nih.gov/ij/ provided by Dr. W. Rasband).

Ca^{2+}-imaging

Intracellular Ca^{2+} was measured with a monochromator-based imaging system consisting of a Polychrome IV monochromator (Till Photonics, Martinsried, Germany) and a Roper Scientific charge-coupled device camera connected to a Axiovert 200M inverted microscope (Zeiss, Gottingen, Germany). The monochromator and camera were controlled by Metafluor software (Version 6.3; Universal Imaging, Downingtown, PA, USA). Cells were loaded with Fura-2 acetoxymethyl ester for 20 min at 37°C. Fluorescence was measured during alternating excitations at 340 and 380 nm. After correction for the individual background fluorescence, the ratio of fluorescence at both wavelengths (F_{340}/F_{380}) was monitored. The standard bathing solution contained (in mM): 90 NaCl, 5 KCl, 1 $MgCl_2$, 2 $CaCl_2$, 10 HEPES, 10 D-glucose, and 110 mannitol, buffered at pH 7.4 with NaOH. For high-Ca^{2+}-containing solution, 90 mM mannitol was replaced with 30 $CaCl_2$.

Statistical analysis

Data are presented as means±SEM of n observations. Statistical differences of the data were evaluated by paired or unpaired Student's t test and were considered significant at $P<0.05$.

Results

Constitutively active TRPP3 channels are voltage-dependent

To characterize the functional properties of murine TRPP3 channels, we performed whole-cell patch-clamp recordings of transiently GFP- and TRPP3-expressing HEK293T cells. In TRPP3-expressing cells, we measured robust channel activity after establishing the whole-cell configuration, whereas no such currents were measured in GFP-expressing cells (Fig. 1a). Although human TRPP3 is reported to be Ca^{2+}-activated [1], we could not observe any difference in current properties when using pipette solutions containing either 10 mM EGTA (with no added Ca^{2+}) or 1 μM free Ca^{2+} (Supplementary Fig. 1). Moreover, we did not detect current activation upon addition of 5 mM Ca^{2+} in the standard bathing solution (Supplementary Fig. 1). These results suggest that Ca^{2+} does not regulate the basal activity of murine TRPP3 channels. TRPP3-expressing cells exhibited outwardly rectifying currents with large tail currents after repolarization to −100 mV. The current–voltage relationships for steady-state currents and tail currents at each test pulse are shown in Fig. 1b. The voltage-dependence of TRPP3 channels was estimated by calculating the apparent open probability (P_o) from tail currents. Tail current amplitudes in function of the prepulse potential were fitted using a modified Boltzmann equation ($I = I_{max}/(1+\exp(-(V-V_{half})/s))$, where V_{half} is the potential of half-maximal activation, s is the slope factor, and I_{max} is the saturating tail current. As shown in Fig. 1c, the constitutive activity of TRPP3 channels is voltage-dependent with a V_{half} of +108.3±20.9 mV and a value for s of 38.0±7.2 mV (n=16). The absolute value of the V_{half} is time-dependent. During an experiment, we observe a constant shift towards more positive potentials. This might be the reason that in the cell-swelling experiments V_{half} values are larger than shown in Fig. 1. Another difficulty is the normalization of the individual tail currents to the maximal tail current amplitude obtained from fitting to the Boltzmann equation in each individual experiment and the impossibility to reach plateau values in long-lasting experiments. We therefore focus the discussion of our results on the shifts in V_{half} rather than absolute values.

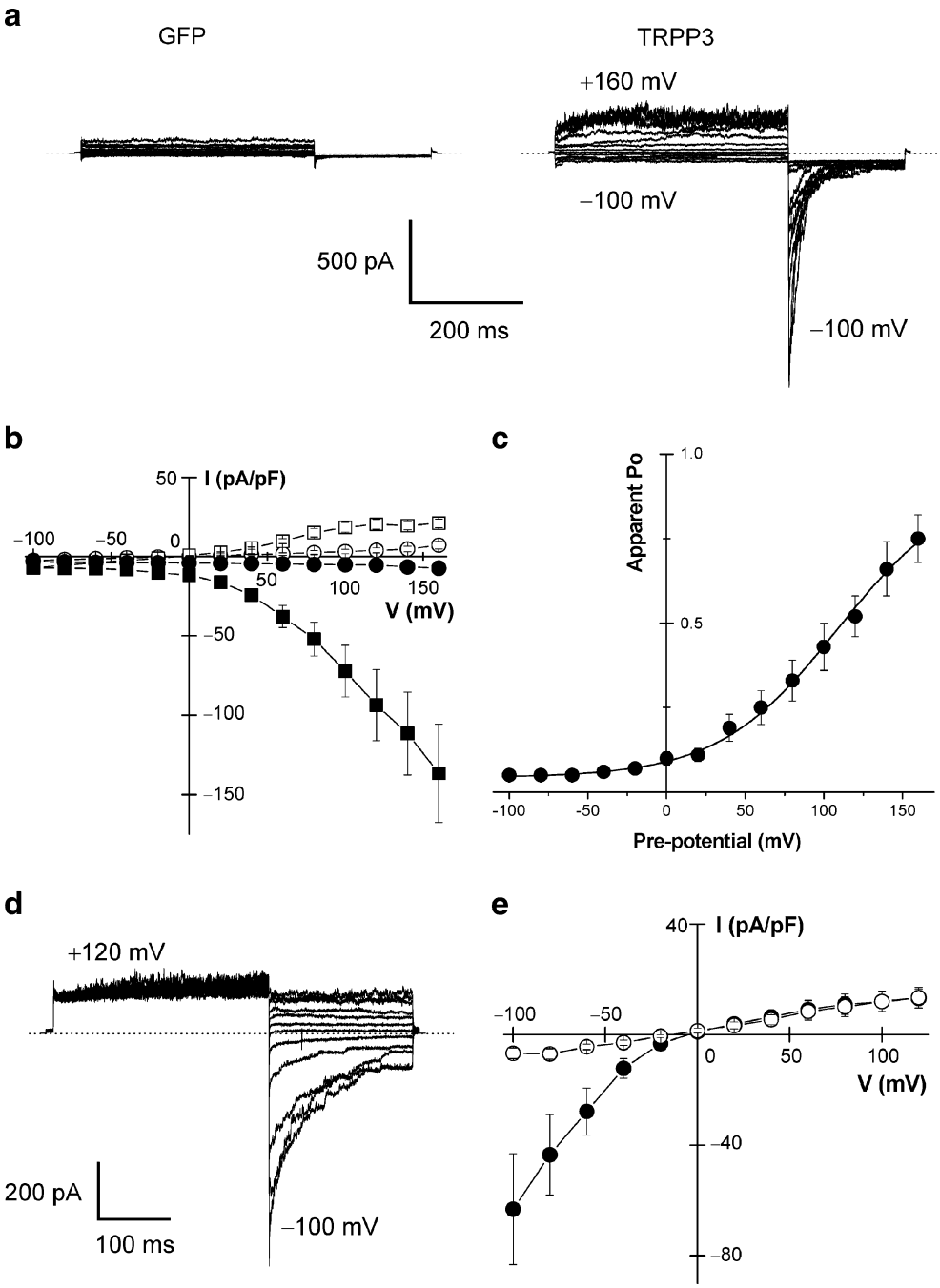

Fig. 1 Voltage dependence of murine TRPP3 channel. **a** Representative whole-cell currents in GFP- and TRPP3-expressing HEK293T cells. Step pulses from −100 to +160 mV in 20 mV increments with a post-pulse to −100 mV were applied. **b** Current–voltage relationships for steady-state currents (*open symbols*) and instantaneous tail currents (*closed symbols*) at each test pulse in GFP- (*circles*; n=4) and TRPP3-expressing HEK293T cells (*squares*; n=16). **c** Voltage dependence of open probabilities (P_o) obtained by normalization of tail currents to the maximal amplitude of each individual cell obtained from Boltzmann fits. The *solid line* indicates the fitting curve. The V_{half} was +108.3±20.9 mV. **d** Representative whole-cell currents elicited by step pulses from −100 to +120 mV in 20 mV increments with a pre-pulse to +120 mV. **e** Current–voltage relationships for steady-state currents (*open*) and instantaneous currents (*closed*). Data are obtained from five experiments. *Dotted lines* in the different panels indicate the zero-current level

To further investigate the voltage dependency of TRPP3 currents, we applied step pulses following a depolarizing pre-pulse to +120 mV. Whereas steady-state currents were outwardly rectifying due to the above-described voltage dependence, the current–voltage relationship for instantaneous TRPP3 currents showed strong inward rectification (Fig. 1d and e). Given that intracellular Mg^{2+} ions are known to cause inward rectifications of other channels, including inwardly rectifying K^+ channels [16] and certain TRP channels [30, 32], we investigated rectification of TRPP3 using Mg^{2+}-free pipette solutions. However, inward rectification and gating kinetics of TRPP3 were not changed when intracellular Mg^{2+} was removed (Fig. 2). In addition, even when we replaced Cs-aspartate by Na-aspartate in the pipette solution, TRPP3 currents displayed inward rectification (Fig. 2).

The kinetics of murine TRPP3 channel activation was further investigated by analyzing the inward tail current amplitude following depolarizing step pulses of different duration to +120 mV. As shown in Fig. 3, the peak tail currents

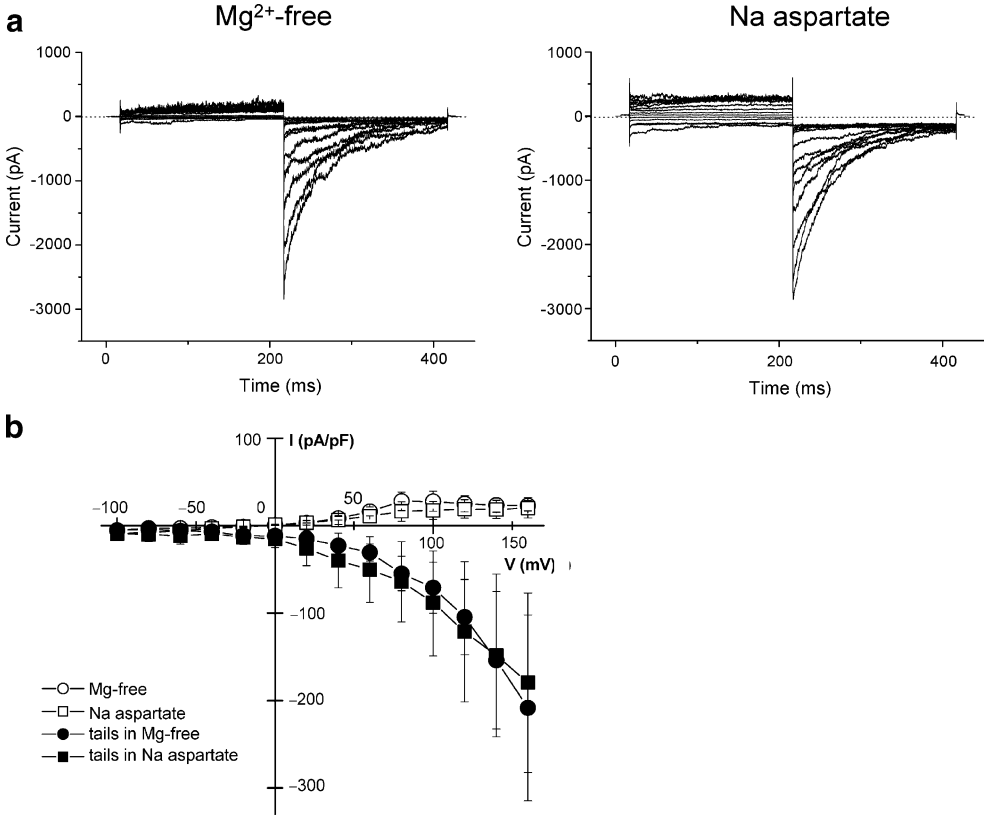

Fig. 2 TRPP3 exhibits inward rectification under intracellular Mg^{2+}-free and symmetrical cationic conditions. **a** Representative whole-cell currents under intracellular Mg^{2+}-free (*left*) and symmetrical cationic conditions (*right*). Currents were obtained from step pulses from −100 to +160 mV in 20-mV increments with a post-pulse to −100 mV. **b** Current–voltage relationships for steady-state currents (*open symbols*) and instantaneous tail currents (*closed symbols*) at each test pulse under intracellular Mg^{2+}-free (*circles*; n=6) and symmetrical cationic conditions (*squares*; n=4) and replacement of Cl^- by aspartate

grew with increasing depolarization, and this time-dependent increase could be described using a monoexponential function with a time constant of 62.3±10.9 ms (n=12).

Ion selectivity and cation blockade of TRPP3 channels

The reversal potential for instantaneous TRPP3 currents was around 0 mV (see Fig. 1e), indicating that the current is cationic given the negative equilibrium potential for Cl– (E_{Cl} −48 mV).

When extracellular Na^+ was completely substituted with Cs^+, $NMDG^+$, or Ca^{2+} reversal potentials were measured using voltage ramps from +100 to −100 mV applied every 5 s. The reversal potentials with Na^+, Cs^+, $NMDG^+$, or Ca^{2+} as main extracellular cation were −8.5±0.8 mV (n=12), −7.6±0.9 mV (n=9), −35.5±3.3 mV (n=9), or −2.0±0.8 mV (n=7), respectively. From the shifts of the reversal potential, we calculated the permeability ratios to Na^+ (P_X/P_{Na}), which yielded the following permeability sequence 3.96±0.33 (Ca)>Cs (1.02±0.02)≈Na (1)>NMDG (0.36±0.04). Results shown in Fig. 4a,b indicate that murine TRPP3 channel is a Ca^{2+}-permeable nonselective cation channel.

Although TRPP3 is permeable to Ca^{2+} and Cs^+, exchanging Na^+ for Ca^{2+} or Cs^+ in the bathing solution reduced inward currents in response to voltage ramps (see Fig. 4a). We measured amplitudes of tail currents induced by step pulses from +120 to −100 mV under these conditions. Extracellular application of Ca^{2+} or Cs^+ reduced tail currents by 86% or 53%, respectively, compared with Na^+ (Fig. 4c,d). Although we observed strong inhibition of TRPP3 tail currents by high Ca^{2+} concentration, the amplitude was significantly different from $NMDG^+$ indicating that Ca^{2+} contributes to the current through TRPP3.

To further confirm Ca^{2+} permeability through TRPP3 channel, we performed Ca^{2+} imaging using Fura-2 in HEK293T cells. We found that the basal Ca^{2+} level was higher in TRPP3-expressing cells than in GFP-expressing cells and that elevation of extracellular Ca^{2+} to 30 mM caused a robust increase of intracellular Ca^{2+} in TRPP3-transfected cells, but not in GFP-expressing cells (Fig. 4e, n=25–26). These results indicate constitutive Ca^{2+} permeability through TRPP3 channels.

Single-channel conductance of TRPP3 channels

Because of the low open probability of TRPP3 at negative potentials and the large amplitude of the single channel currents, we could reliably measure single-channel activity in whole-cell recordings. Typical recordings of the constitutive channel activity are shown in Fig. 5a. Similar single-channel currents were never observed in GFP-

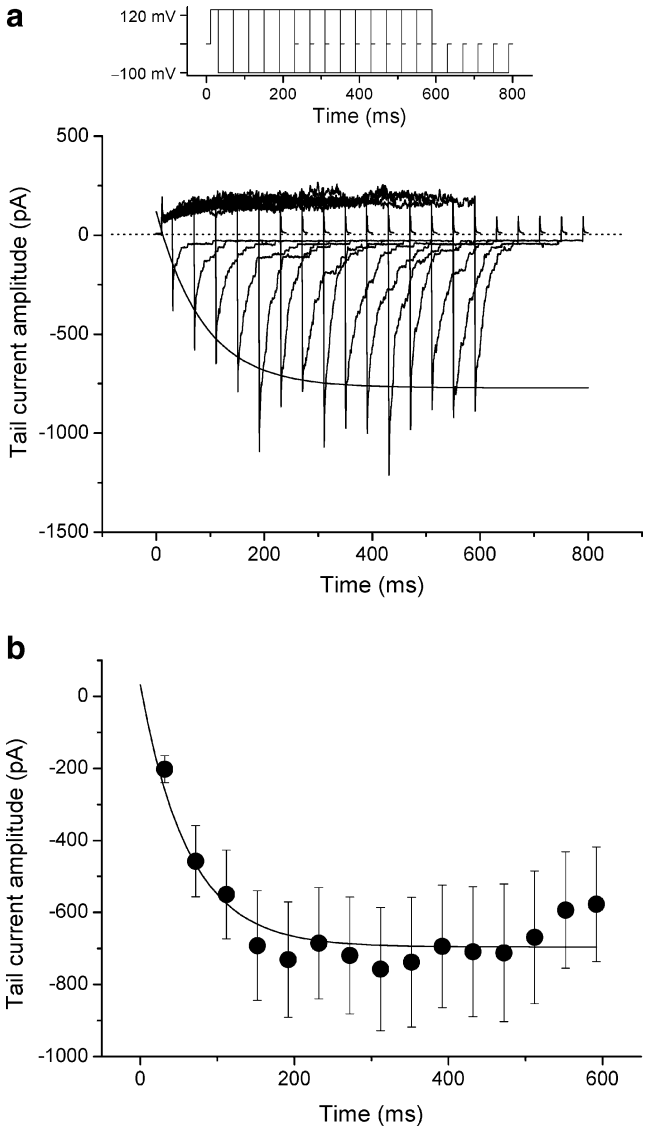

Fig. 3 Kinetics of voltage-dependent activation of murine TRPP3. **a** Representative whole-cell current evoked by the indicated step pulses. **b** Averaged tail current amplitudes from 12 experiments. The *solid line* represents the monoexponential fit of peak tail current amplitudes, which yielded a time constant of 62.3±10.9 ms in 12 experiments

expressing cells (n=12; data not shown). The single-channel slope conductance of TRPP3 channels at negative potentials was 184±5 pS (n=8–16; Fig. 5b), indicating that murine TRPP3 is a cation channel with a large single-channel conductance.

Due to the high open probability, we could not reliably measure single-channel TRPP3 activity at positive potentials in the whole-cell configuration. However, we could observe outward single-channel currents at potentials more depolarized than +100 mV in six of 52 cell-attached recordings, with a single-channel slope conductance at positive potentials of 105±3 pS (Fig. 5c,d). Such single-channel activity was never observed in GFP-expressing cells (n=32). Whereas steady-state inward single-channel TRPP3 currents were never detected in cell attached patches, deactivating single-channel TRPP3 currents were consistently observed at −100 mV following depolarizing voltage steps that evoked outward current. The single-channel amplitude at −100 mV in cell-attached recordings was similar to that in whole-cell recordings, suggesting that this channel activity is mediated by TRPP3 channels and indicating that TRPP3 exhibits inward rectification at the single-channel level.

Acid sensitivity of TRPP3 channels

Since it has been suggested that heteromultimers of PKD1L3 and TRPP3 function as sour receptors [9, 10, 15], we examined effects of citric acid on TRPP3 channels. In TRPP3-expressing cells, spontaneous single-channel TRPP3 currents at a holding potential of −60 mV could be reliably recorded in whole-cell conditions for more than 20 min (data not shown). Figure 6a shows a typical holding current at −60 mV, illustrating the effect of adding solution containing 25 mM citric acid (pH 2.7). Single-channel TRPP3 currents disappeared during application of citric acid, although a sharp transient inward current was consistently observed. After restoration of normal pH, the TRPP3 currents recovered. The transient acid-induced current was blocked by 100 μM amiloride or by replacement of NaCl with CsCl in bathing solutions (data not shown, n=8 or 4, respectively) and was also observed in non-transfected HEK293 cells, which indicates that it is carried by the endogenously expressed acid-sensitive ion channel (ASIC) [6]. As shown in Fig. 6b, c, tail currents of TRPP3 channel were completely and reversibly inhibited by acidification with citric acid. These results indicate that strong acidification with citric acid suppresses TRPP3 currents. Surprisingly, alkalization to pH 9 strongly enhanced TRPP3 tail currents (Fig. 6d, e). These results indicate that murine TRPP3 channels are sensitive to pH changes. However, the effects of acidification and alkalization are opposite to what has been reported for the TRPP3/PKD1L3 complexes [9, 10].

Volume sensitivity of TRPP3 channels

It has been previously demonstrated, using Ca^{2+} imaging, that hypotonic stimuli evoke transient increases in intracellular Ca^{2+} concentration in HEK293 cells coexpressing TRPP1 and TRPP3 [17]. However, no electrophysiological data exists proving directly modulation of TRPP3 channels by osmotic stimuli. Therefore, we focused on the effects of cell volume changes on TRPP3 currents. Figure 7a shows the correlation between TRPP3 currents and cell volume.

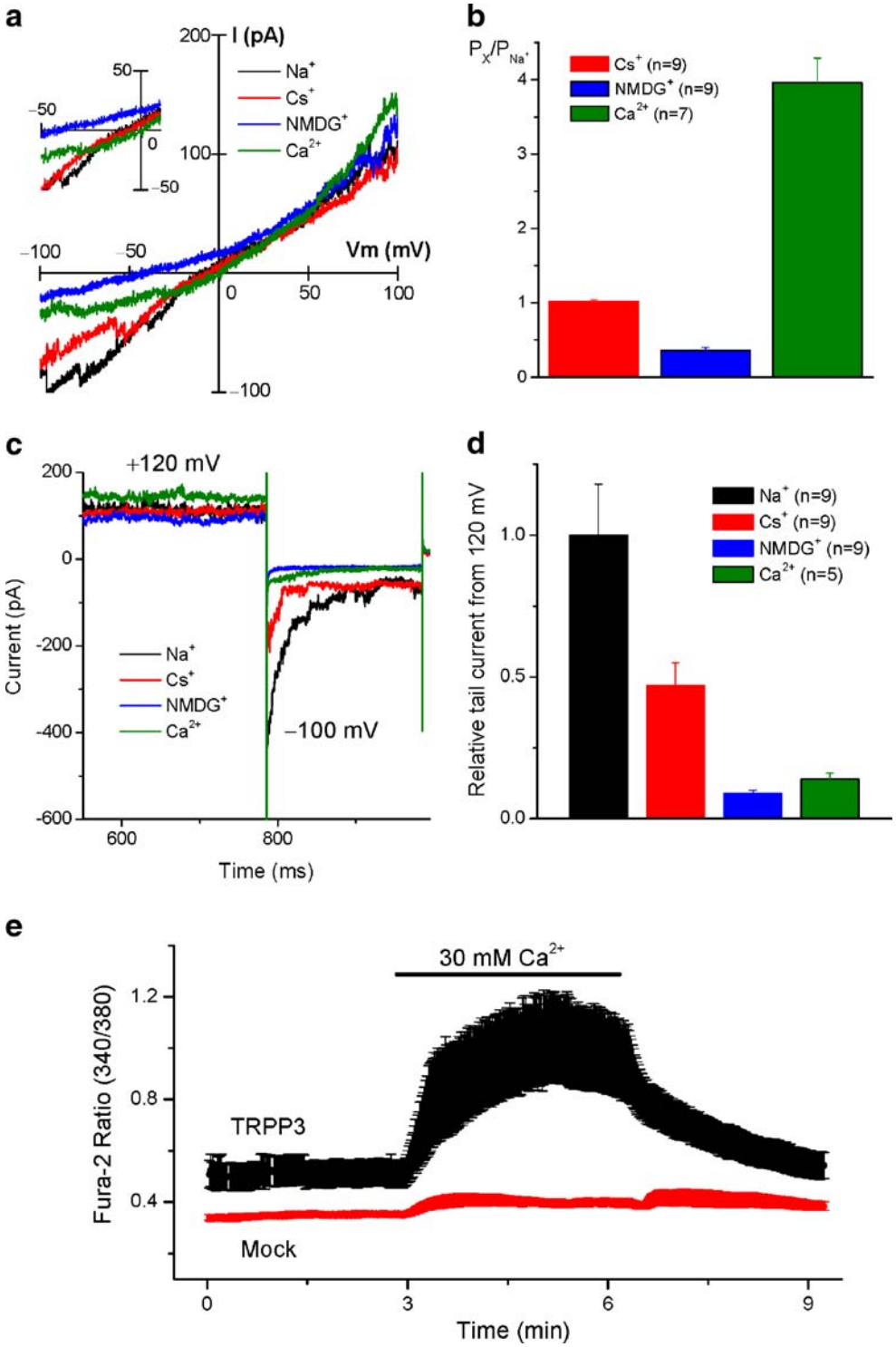

Fig. 4 Ion selectivity and conductivity of murine TRPP3. **a** Representative whole-cell currents were obtained using ramp pulses of 100 ms from +100 to −100 mV in different bathing solutions containing Na^+, Cs^+, $NMDG^+$, or Ca^{2+} as the only permeant cation species. *Inset* zooms in on the reversal potentials. **b** Summarized relative cation permeability to Na^+. **c** Representative whole-cell currents showing changes of the tail current amplitude by different cations in the same conditions as (**a**). Currents were recorded using step pulses from +120 to −100 mV. **d** Summarized relative cation conductivity to Na^+. **e** Averaged ratiometric intracellular Ca^{2+} response to a rise in extracellular Ca^{2+} concentration in GFP- and TRPP3-transfected cells (n=26 and 25, respectively)

After application of hypotonic solution in TRPP3-expressing cells, TRPP3 currents recorded at −60 mV increased gradually. The current changes were closely correlated to changes in cell volume. Subsequent application of hypertonic solution resulted in cell shrinkage and a concomitant decrease in TRPP3 currents. In contrast, GFP-expressing cells did not show similar channel activation after cell swelling (data not shown).

To examine how cell volume changes modulate TRPP3 currents, we analyzed TRPP3 single-channel properties during cell volume changes. Figure 7b shows typical traces with the corresponding amplitude histograms. We found

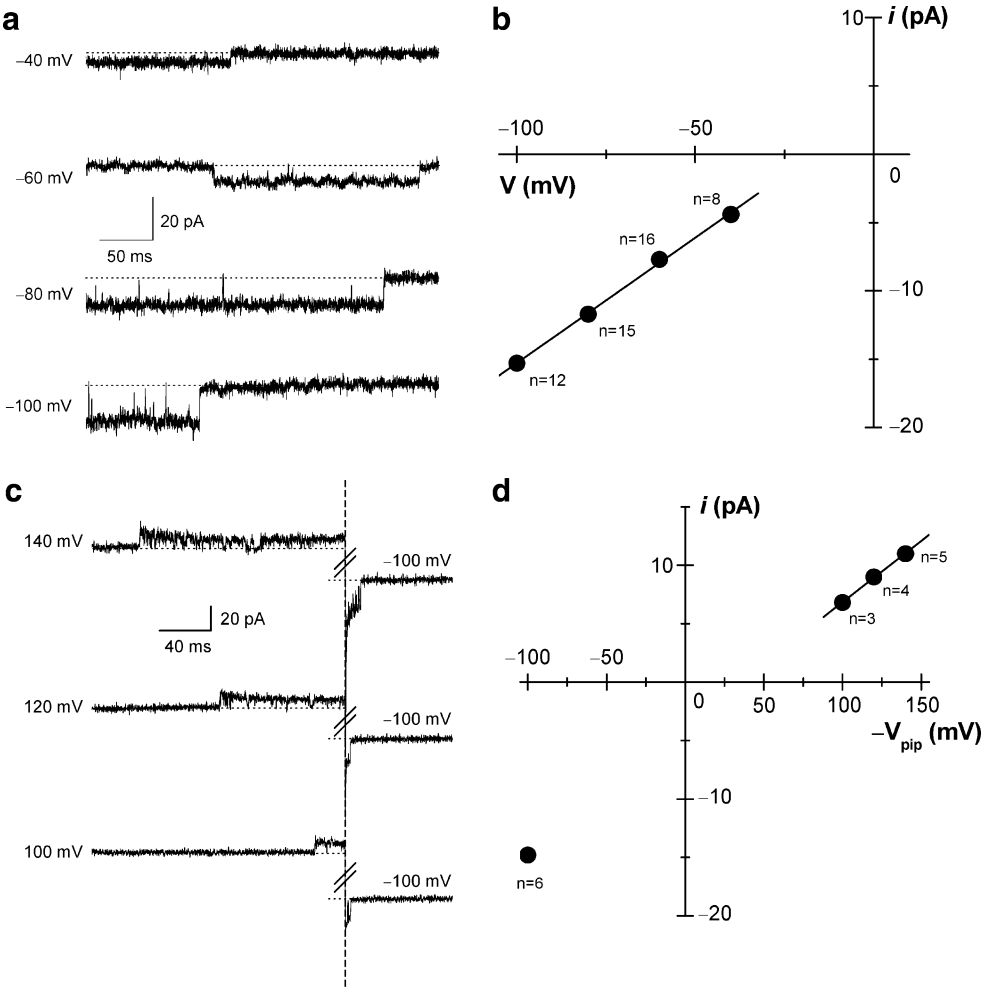

Fig. 5 Single-channel activity of murine TRPP3 channel in whole-cell (**a** and **b**) and cell-attached (**c** and **d**) recordings. **a** Representative single-channel activities at negative potentials between −40 and −100 mV as indicated. The closed level in each recording is indicated by a *dotted line*. **b** Current–voltage relationships for unitary current amplitude (*i*). The single-channel slope conductance at negative potentials was 184±5 pS in eight to 16 experiments. **c** Representative single-channel activities at positive potentials between +100 and +140 mV and at −100 mV as indicated. **d** Current–voltage relationships for the unitary current amplitude (*i*). The single-channel slope conductance at positive potentials was 105±3 pS in three to five experiments

that cell swelling increased the channel activity (NP_o) of TRPP3 channels in a reversible manner (Fig. 7c). Single-channel amplitudes at −60 mV were not significantly altered during cell volume changes (Fig. 7d). These results suggest that cell volume changes regulate the open probability of TRPP3 channels, but not the single-channel conductance.

Next, we investigated the modulation of the voltage dependence of TRPP3 channels by osmotic stimuli at the whole-cell level. As shown in Fig. 8, cell swelling increased outward currents at more positive potentials than +100 mV and the corresponding tail currents at −100 mV, whereas cell shrinkage had the opposite effect (Fig. 8a–c). As shown in Fig. 6d, the voltage dependence of TRPP3 channels was shifted leftward and rightward by cell swelling and cell shrinkage, respectively. The voltage for half-maximal activation (V_{half}) changed from 194.6±6.0 mV (n=8) over 119.3±3.4 mV (n=8) to 217.2±6.0 mV (n=4) in isotonic, hypotonic, and hypertonic conditions respectively. Thus, changes in cell volume affect the voltage-dependent gating of TRPP3 channels.

It has been previously demonstrated that cell swelling activates TRPV4 via phospholipase A_2 (PLA_2)-dependent formation of arachidonic acid [33]. To test whether a similar mechanism may mediate the influence of cell volume on TRPP3, we first tested the effect of a nonselective PLA_2 inhibitor, 4-bromophenacyl bromide (pBPB), on TRPP3 activity. In TRPP3-transfected cells pretreated with 100 μM pBPB for 30 min, we could no longer detect TRPP3 channel activity (data not shown). Moreover, we found that application of 10 μM arachidonic acid increased the TRPP3 tail currents and shifted the voltage dependence of TRPP3 channels. V_{half} changed from 154.7±0.9 mV before to 107.9±1.0 mV after application of arachidonic acid, respectively (n=6; Fig. 9).

Discussion

This study is the first characterization of electrophysiological properties of murine TRPP3 channels using whole-cell patch-clamp recordings. When murine TRPP3

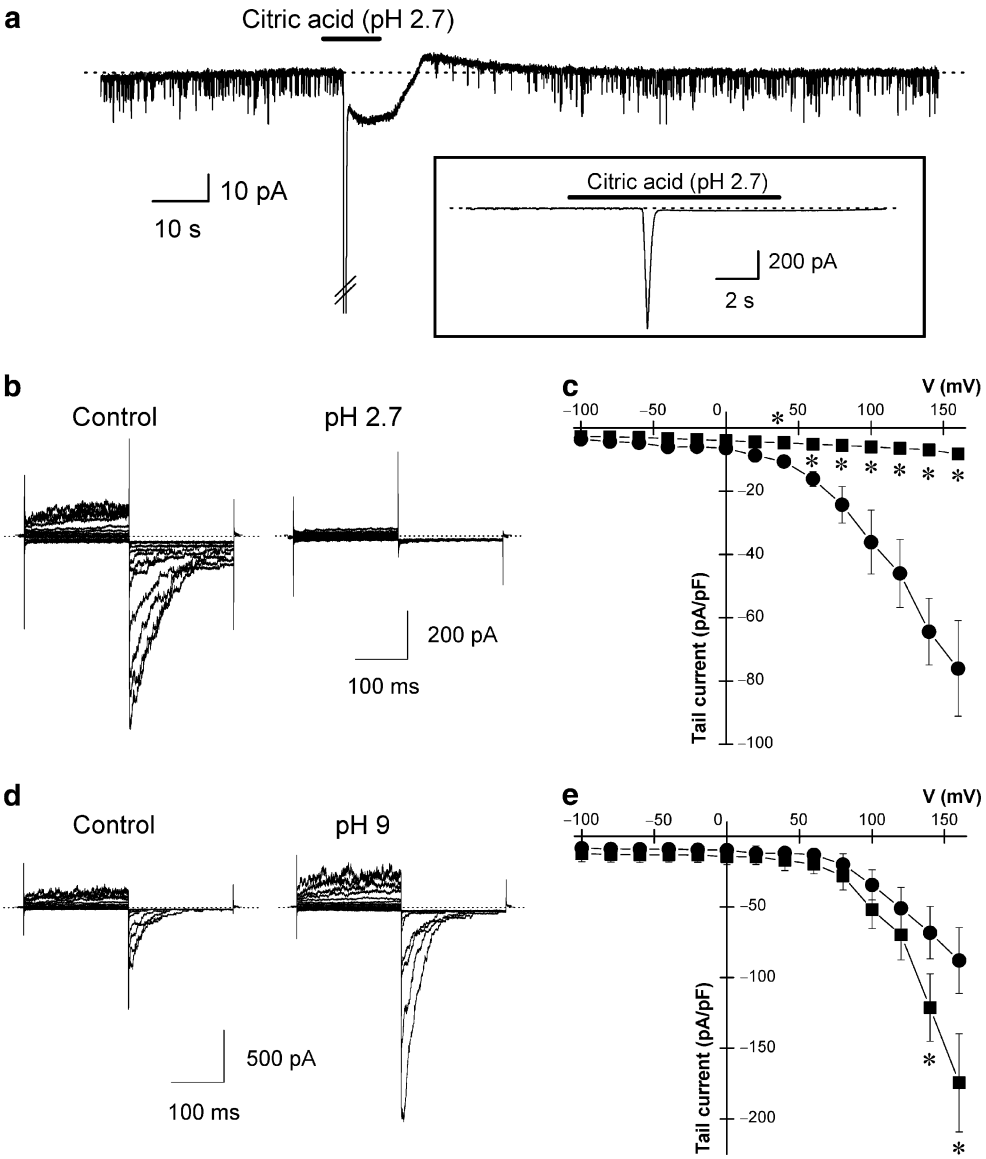

Fig. 6 Murine TRPP3 channels are inhibited by acidification. **a** Representative macroscopic currents at −60 mV in whole-cell recordings. The typical endogenous acid-sensitive current is shown in *inset* (same cell). Applications of acidic solutions containing 25 mM citric acid are indicated by *horizontal bars*. Note that basal holding currents changed during acidification, which we attribute to acid-activated Cl^- currents. **b** Representative whole-cell currents before and during acidification. Currents were obtained from step pulses from −100 to −140 mV in 20-mV increments with a post-pulse to −100 mV. **c** Current–voltage relationships for instantaneous tail currents at each test pulse before (*circles*) and during acidification (*squares*). Data are obtained from five experiments. **d** Representative whole-cell currents before and during alkalization. Currents were obtained from step pulses from −100 to +160 mV in 20-mV increments with a post-pulse to -100 mV. **e** Current–voltage relationships for instantaneous tail currents at each test pulse before (*circles*) and during alkalization (*squares*). Data are obtained from eight experiments

was overexpressed in HEK293T cells, we could observe spontaneously active nonselective TRPP3 channel activity. The TRPP3 channel exhibited large single-channel conductance, significant Ca^{2+} permeability, and voltage-dependent activation. Moreover, we found that cell swelling increased TRPP3 currents, whereas cell shrinkage reduced them.

It has been reported that human TRPP3 forms a nonselective cation channel when it is expressed in *Xenopus* oocytes [1–3, 14], planar lipid bilayers [13], or mammalian cells [25]. The human TRPP3 channel is considered to be Ca^{2+}-activated [1], although no functional consequence of this Ca^{2+} regulation has been reported [25]. In the present study, changes in the intracellular or extracellular Ca^{2+} concentration were without any effect, suggesting that murine TRPP3 is not regulated by Ca^{2+}. Identification of the Ca^{2+}-binding sites responsible for Ca^{2+}-induced activation of human TRPP3 may help to understand the apparent difference with murine TRPP3. It has been demonstrated that an EF-hand in human TRPP3 is not the determinant for the Ca^{2+}-activation [13].

The human TRPP3 channel shows constitutive activity and a large single-channel conductance (67–399 pS), depending on the ionic conditions [2, 25]. For human TRPP3, the reported Ca^{2+} permeability is higher than the permeability for small monovalent cations such as Na^+ [1]. In line herewith, we measured a single-channel slope conductance of murine TRPP3 channels of 184 pS at negative potentials and an ion selectivity sequence $Ca^{2+} \gg Cs^+ \approx Na^+ \gg NMDG^+$. We observed a different sequence ($Na^+ > Cs^+ > Ca^{2+}$) for the ion conductivity of murine TRPP3 channels. This is consistent with previous data on

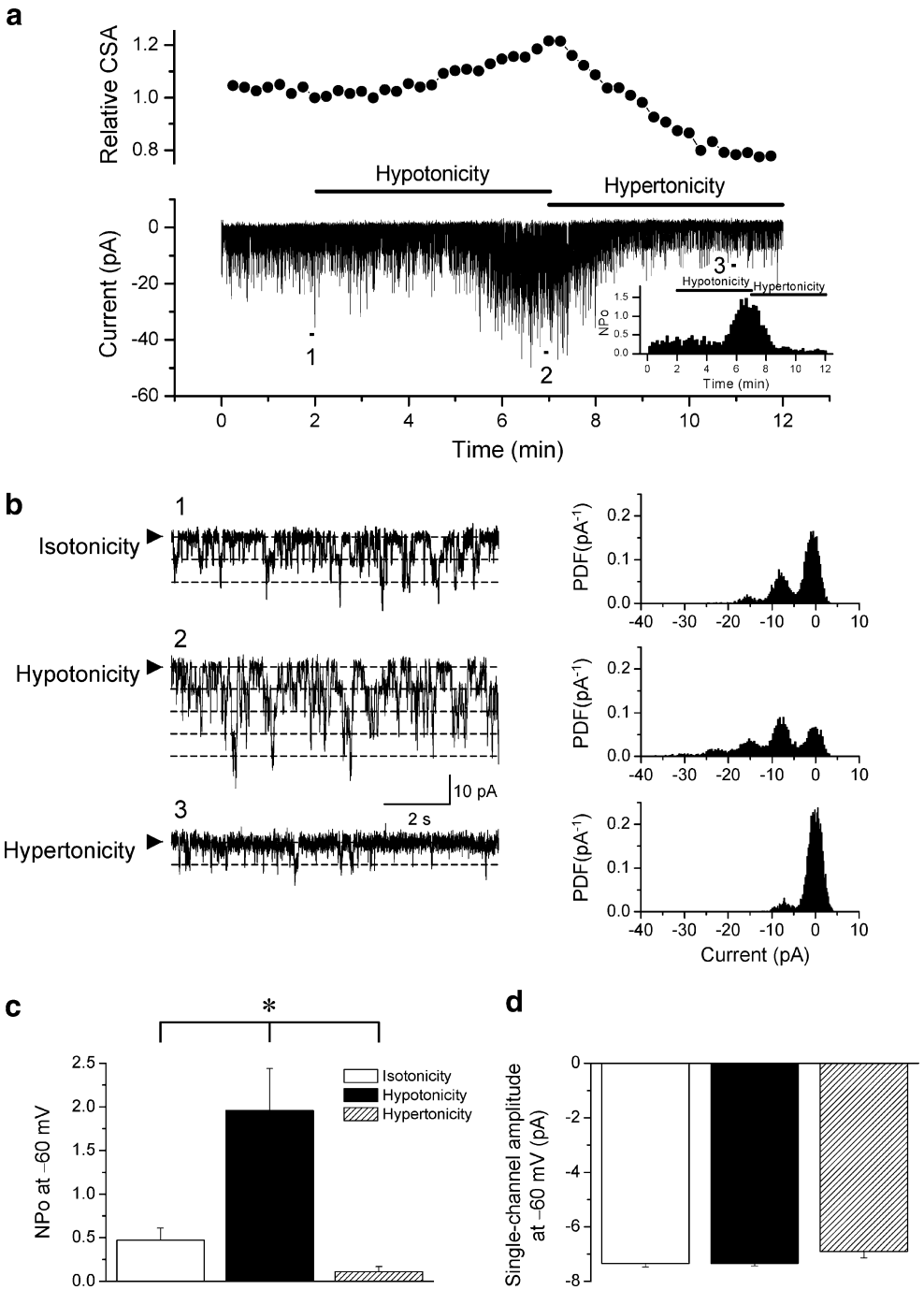

Fig. 7 Effects of osmotic swelling on single-channel TRPP3 activity. **a** Representative time courses of relative cross-sectional area (CSA; *upper panel*) and inward currents at −60 mV (*bottom panel*). Experiments were performed in the whole-cell configuration. *Inset*: time course of the corresponding channel activities (NPo). Applications of hypotonic and hypertonic solutions are indicated by *horizontal bars*. The measured CSA of a single cell was normalized to the CSA immediately before application of hypotonic solution. **b** Time-expanded traces during different osmotic stimuli designated by 1, 2, and 3 in (**a**). *Arrowheads* indicate the closed level. The corresponding all-points amplitude histograms are shown on the *right*. *PDF* Probability density function. **c** and **d** Effects of osmotic stimuli on NPo (**c**) and single-channel amplitudes (**d**) at −60 mV. The data are averaged from six to ten experiments

human TRPP3 channels, which showed an inverse correlation between ion conductivity for monovalent cations and ion radius [2], and a smaller single-channel conductance for Ca^{2+} than for Na^{+} [25]. Furthermore, the present study shows that the current–voltage relationship for instantaneous tail currents of murine TRPP3 channels was inwardly rectifying. The rectification was not due to asymmetrical cationic conditions because replacing Cs-aspartate with Na-aspartate in pipette solutions resulted in a similar current–voltage relationship. Rather, the result suggests that the pore of murine TRPP3 exhibits intrinsic inward rectification. We observed inward-rectifying single-channel TRPP3 currents in cell-attached patches, which is in accordance with previous data for human TRPP3 [14]. Thus, with respect to single-channel conductance, ion selectivity, and rectification, the murine TRPP3 channel exhibits similar pore properties than the human TRPP3 channel. However, pore mutation experiments would be needed to fully

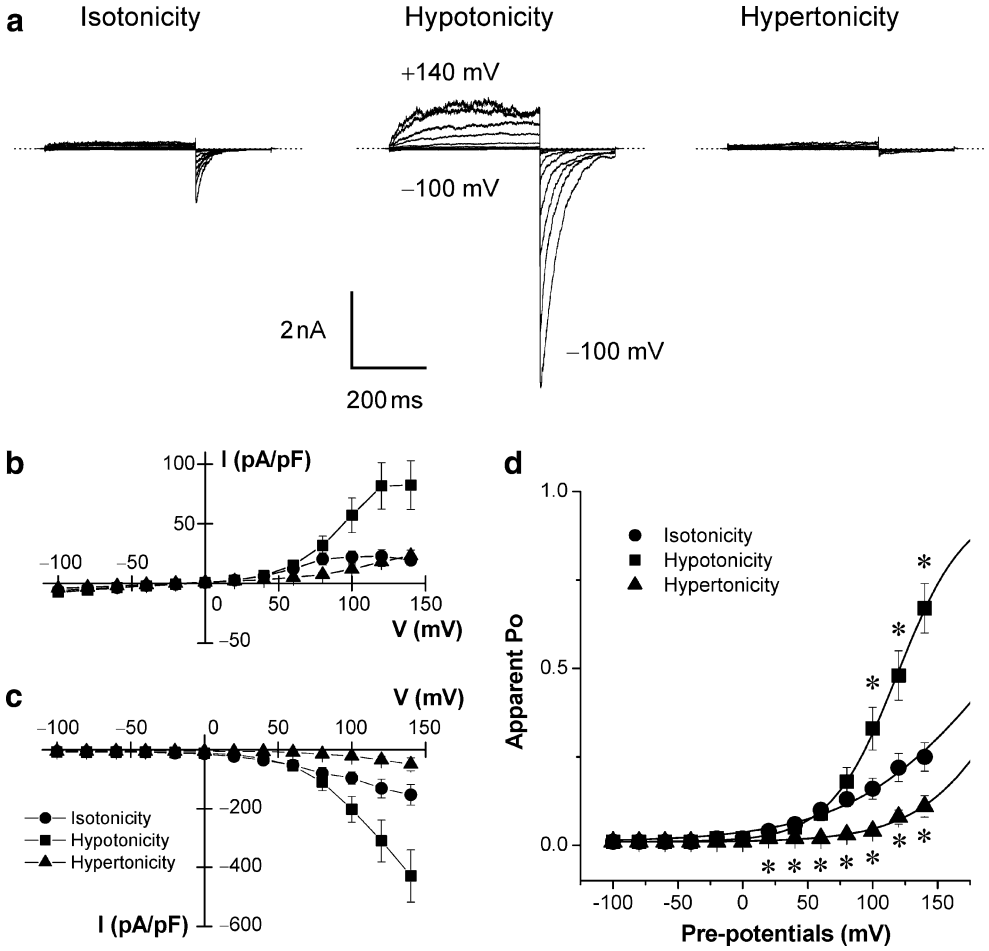

Fig. 8 Volume sensitivity of murine TRPP3 channel at the whole-cell level. **a** Representative whole-cell currents in response to osmotic stimuli. Currents were obtained from step pulses from −100 to +140 mV in 20-mV increments with a post-pulse to −100 mV. **b** Current–voltage relationships for steady-state currents under isotonic (*circles*; n=8), hypotonic (*squares*; n=8), and hypertonic (*triangles*; n=4) conditions. **c** Current–voltage relationships for instantaneous tail currents at each test pulse under osmotic stimuli. **d** Voltage dependence of P_o during different osmotic conditions. *Solid lines* represent a Boltzmann function fit to the data. The shifts in V_{half} were +75.3± 4.8 mV (*leftward*) for changes from isotonic to hypotonic and −22.6±4.7 mV (*rightward*) for changes from isotonic to hypertonic conditions, respectively

establish that the overexpressed TRPP3 actually forms the ion-conducting pore of the channels that underlie the macroscopic and single-channel currents.

We also observed voltage-dependent activation of murine TRPP3 channels. Here, repolarization after depolarization caused large transient inward TRPP3 tail currents. The channel activities calculated from tail currents were increased with stronger or longer depolarizations. We found that murine TRPP3 channels exhibit a voltage dependence with a low apparent gating charge (<1 equivalent charge), comparable to the small gating charges found in other voltage-dependent TRP channels [19, 20, 29, 31]. Despite the growth of inward tail currents following increasingly depolarizing steps, we observed only small activation of outward TRPP3 currents. We could exclude the possibility that the small outward currents reflect inhibition by intracellular Mg^{2+} because outward currents remained small even when Mg^{2+}-free pipette solutions were used. The human TRPP3 channel is reportedly activated by hyperpolarization [14] in contrast to our current findings with the murine TRPP3 clone. The reason for this discrepancy is not known.

The gating behavior of TRPP3 is somewhat reminiscent of that of the human *ether-à-go-go*-related gene (HERG) K^+ channels, which play an important role in the repolarization of the heart [27, 34]. Indeed, both TRPP3 and HERG are activated by depolarization yet carry little outward current. However, upon repolarization, both channels enable large tail currents. In the case of HERG channels, inward rectification is due to a rapid C-type inactivation mechanism that prevents outward current during depolarization. During subsequent repolarization, HERG channels recover rapidly from inactivation but deactivate slowly, resulting in a large tail currents. Although C-type inactivation has not yet been described in TRP channels, it is tempting to speculate that a similar mechanism may be at work in TRPP3 channels. Independent of the underlying mechanism, the gating behavior of TRPP3 could be important in excitable cells, where TRPP3 channels would carry a depolarizing current during the repolarizing phase of an action potential.

We furthermore investigated whether cell volume changes affect murine TRPP3 currents and found a strong increase. Cell swelling shifted the voltage dependency to

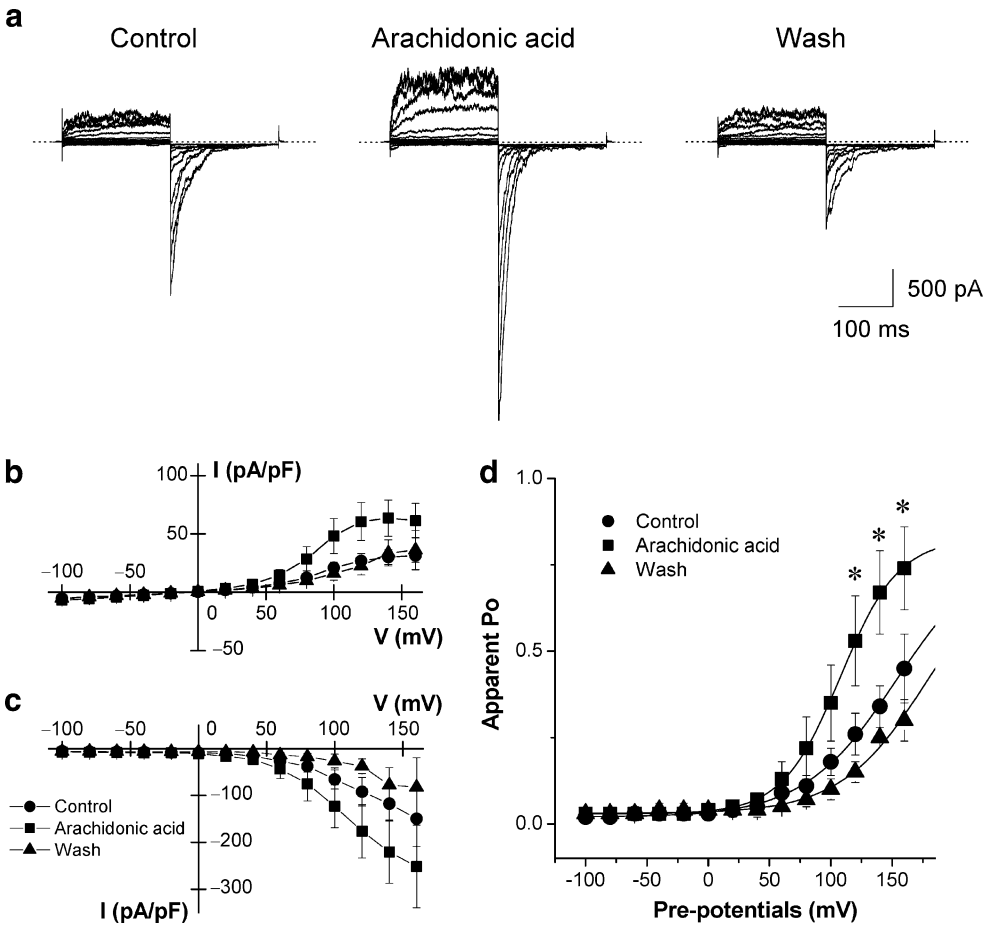

Fig. 9 Effects of arachidonic acid on murine TRPP3. **a** Representative whole-cell currents before, during, and after application of 10 μM arachidonic acid. Currents were measured during step pulses from −100 to +160 mV in 20-mV increments with a post-pulse to −100 mV. **b** Corresponding current–voltage relations **c** Current–voltage relationships for instantaneous tail currents at each test pulse under different conditions. **d** Voltage dependence of P_o. *Solid lines* represent a Boltzmann function fit to the data. V_{half} before and during application of arachidonic acid was 154.7±0.9 or 107.9±1.0 mV, respectively. Data are obtained from six experiments

more negative potentials, while cell shrinkage caused a positive shift of the voltage-dependent activation. Similarly, activation of several TRP channels is correlated with a shift of the voltage-dependent activation curve [20, 30]. There was a clear delay between the changes in extracellular osmolality and the resulting alterations of TRPP3 channel activity, indicating that the TRPP3 channel does not act as a direct sensor of osmotic strength. In contrast, there was a tight correlation between cell volume and TRPP3 currents, suggesting that TRPP3 channels are directly or indirectly modulated by cell volume changes. PLA_2-dependent signals such as arachidonic acid are known to be involved in the activation of TRPV4 by cell swelling [33, 35]. A similar mechanism may be at work during swelling-induced activation of TRPP3 channels, as application of arachidonic acid enhanced TRPP3 channel activity, whereas inhibition of PLA_2 using pBPB inhibited channel activity. Further studies are required to understand how murine TRPP3 channel is modulated by arachidonic acid.

It has been reported that coexpression of murine TRPP3 with PKD1 (TRPP1)-like proteins results in a translocation of TRPP3 channels from the ER to the cell surface and formation of functional cation channels that are sensitive to stimuli such as cell swelling and sour taste compounds [10, 17]. In the present study, however, we observed osmotic regulation on TRPP3 channels without coexpression of human TRPP1. Therefore, we conclude that murine TRPP3 channel by itself is functionally regulated by cell volume changes, although our data do not exclude that coexpression of TRPP1 might increase the volume sensitivity of murine TRPP3 channels. In addition, we demonstrated that strong acidification with citric acid inhibited TRPP3 currents. This result is consistent with the previous data showing that low extracellular pH decreases the basal human TRPP3 conductance [1]. Moreover, we found that alkalization caused an increase in tail currents of murine TRPP3 channel. As such, the behavior of murine TRPP3 channels is completely opposite to sour receptors reported in PKD1L3/TRPP3 coexpressing cells [10]. These results mandate further investigation into the regulation of murine TRPP3 channels by PKD1 (TRPP1)-like proteins.

In summary, here, we demonstrate that murine TRPP3 is a constitutively active, voltage-dependent and Ca^{2+}-permeable nonselective cation channel, whose activity is modulated by pH and cell volume. The physiological role of TRPP3 remains to be unraveled.

Acknowledgement We thank Dr. Matsunami for providing the murine TRPP3 cDNA. We also thank all members of the Leuven laboratory for helpful suggestions and criticisms. This work was supported by grants from the Human Frontiers Science Program (HFSP Research Grant Ref. RGP 32/2004), Interuniversity Attraction Poles Programme-Belgian State-Belgian Science Policy, P6/28, and the Flemish Government (Excellentiefinanciering EF/95/010), Novartis, the Uehara Memorial Foundation, and Kanae Foundation for the promotion of medical science.

References

1. Chen XZ, Vassilev PM, Basora N, Peng JB, Nomura H, Segal Y, Brown EM, Reeders ST, Hediger MA, Zhou J (1999) Polycystin-L is a calcium-regulated cation channel permeable to calcium ions. Nature 401:383–386
2. Dai XQ, Karpinski E, Chen XZ (2006) Permeation and inhibition of polycystin-L channel by monovalent organic cations. Biochim Biophys Acta 1758:197–205
3. Dai XQ, Ramji A, Liu Y, Li Q, Karpinski E, Chen XZ (2007) Inhibition of TRPP3 channel by amiloride and analogs. Mol Pharmacol 72:1576–1585
4. Delmas P, Padilla F, Osorio N, Coste B, Raoux M, Crest M (2004) Polycystins, calcium signaling, and human diseases. Biochem Biophys Res Commun 322:1374–1383
5. Giamarchi A, Padilla F, Coste B, Raoux M, Crest M, Honore E, Delmas P (2006) The versatile nature of the calcium-permeable cation channel TRPP2. EMBO Rep 7:787–793
6. Gunthorpe MJ, Smith GD, Davis JB, Randall AD (2001) Characterisation of a human acid-sensing ion channel (hASIC1a) endogenously expressed in HEK293 cells. Pflügers Arch 442:668–74
7. Hanaoka K, Qian F, Boletta A, Bhunia AK, Piontek K, Tsiokas L, Sukhatme VP, Guggino WB, Germino GG (2000) Co-assembly of polycystin-1 and -2 produces unique cation-permeable currents. Nature 408:990–994
8. Hille B (1972) The permeability of the sodium channel to metal cations in myelinated nerve. J Gen Physiol 59:637–658
9. Huang AL, Chen X, Hoon MA, Chandrashekar J, Guo W, Trankner D, Ryba NJ, Zuker CS (2006) The cells and logic for mammalian sour taste detection. Nature 442:934–938
10. Ishimaru Y, Inada H, Kubota M, Zhuang H, Tominaga M, Matsunami H (2006) Transient receptor potential family members PKD1L3 and PKD2L1 form a candidate sour taste receptor. Proc Natl Acad Sci USA 103:12569–12574
11. Lambert S, Oberwinkler J (2005) Characterization of a proton-activated, outwardly rectifying anion channel. J Physiol 567:191–213
12. Lewis CA (1979) Ion-concentration dependence of the reversal potential and the single channel conductance of ion channels at the frog neuromuscular junction. J Physiol 286:417–445
13. Li Q, Dai XQ, Shen PY, Wu Y, Long W, Chen CX, Hussain Z, Wang S, Chen XZ (2007) Direct binding of alpha-actinin enhances TRPP3 channel activity. J Neurochem 103:2391–2400
14. Liu Y, Li Q, Tan M, Zhang YY, Karpinski E, Zhou J, Chen XZ (2002) Modulation of the human polycystin-L channel by voltage and divalent cations. FEBS Lett 525:71–76
15. LopezJimenez ND, Cavenagh MM, Sainz E, Cruz-Ithier MA, Battey JF, Sullivan SF (2006) Two members of TRPP family of ion channels, Pkd1l3 and Pkd2l1, are co-expressed in a subset of taste receptor cells. J Neurochem 98:68–77
16. Matsuda H, Saigusa A, Irisawa H (1987) Ohmic conductance through the inwardly rectifying K channel and blocking by internal Mg^{2+}. Nature 325:156–159
17. Murakami M, Ohba T, Xu F, Shida S, Satoh E, Ono K, Miyoshi I, Watanabe H, Ito H, Iijima T (2005) Genomic organization and functional analysis of murine PKD2L1. J Biol Chem 280:5626–5635
18. Nilius B, Owsianik G, Voets T, Peters JA (2007) Transient receptor potential cation channels in disease. Physiol Rev 87:165–217
19. Nilius B, Prenen J, Droogmans G, Voets T, Vennekens R, Freichel M, Wissenbach U, Flockerzi V (2003) Voltage dependence of the Ca^{2+}-activated cation channel TRPM4. J Biol Chem 278:30813–30820
20. Nilius B, Talavera K, Owsianik G, Prenen J, Droogmans G, Voets T (2005) Gating of TRP channels: a voltage connection? J Physiol 567:35–44
21. Nomura H, Turco AE, Pei Y, Kalaydjieva L, Schiavello T, Weremowicz S, Ji W, Morton CC, Meisler M, Reeders ST, Zhou J (1998) Identification of PKDL, a novel polycystic kidney disease 2-like gene whose murine homologue is deleted in mice with kidney and retinal defects. J Biol Chem 273:25967–25973
22. Qamar S, Vadivelu M, Sandford R (2007) TRP channels and kidney disease: lessons from polycystic kidney disease. Biochem Soc Trans 35:124–128
23. Ramsey IS, Delling M, Clapham DE (2006) An introduction to TRP channels. Annu Rev Physiol 68:619–647
24. Sutters M, Germino GG (2003) Autosomal dominant polycystic kidney disease: molecular genetics and pathophysiology. J Lab Clin Med 141:91–101
25. Sutton KA, Jungnickel MK, Ward CJ, Harris PC, Florman HM (2006) Functional characterization of PKDREJ, a male germ cell-restricted polycystin. J Cell Physiol 209:493–500
26. Trouet D, Nilius B, Voets T, Droogmans G, Eggermont J (1997) Use of a bicistronic GFP-expression vector to characterise ion channels after transfection in mammalian cells. Pflügers Arch 434:632–638
27. Vandenberg JI, Torres AM, Campbell TJ, Kuchel PW (2004) The HERG K^+ channel: progress in understanding the molecular basis of its unusual gating kinetics. Eur Biophys J 33:89–97
28. Venkatachalam K, Montell C (2007) TRP channels. Annu Rev Biochem 76:387–417
29. Voets T, Droogmans G, Wissenbach U, Janssens A, Flockerzi V, Nilius B (2004) The principle of temperature-dependent gating in cold- and heat-sensitive TRP channels. Nature 430:748–754
30. Voets T, Janssens A, Prenen J, Droogmans G, Nilius B (2003) Mg^{2+}-dependent gating and strong inward rectification of the cation channel TRPV6. J Gen Physiol 121:245–260
31. Voets T, Owsianik G, Janssens A, Talavera K, Nilius B (2007) TRPM8 voltage sensor mutants reveal a mechanism for integrating thermal and chemical stimuli. Nat Chem Biol 3:174–182
32. Voets T, Prenen J, Fleig A, Vennekens R, Watanabe H, Hoenderop JG, Bindels RJ, Droogmans G, Penner R, Nilius B (2001) CaT1 and the calcium release-activated calcium channel manifest distinct pore properties. J Biol Chem 276:47767–47770
33. Vriens J, Watanabe H, Janssens A, Droogmans G, Voets T, Nilius B (2004) Cell swelling, heat, and chemical agonists use distinct pathways for the activation of the cation channel TRPV4. Proc Natl Acad Sci USA 101:396–401
34. Wang S, Liu S, Morales MJ, Strauss HC, Rasmusson RL (1997) A quantitative analysis of the activation and inactivation kinetics of HERG expressed in *Xenopus* oocytes. J Physiol 502:45–60
35. Watanabe H, Vriens J, Prenen J, Droogmans G, Voets T, Nilius B (2003) Anandamide and arachidonic acid use epoxyeicosatrienoic acids to activate TRPV4 channels. Nature 424:434–8